

SCIENTIFIC REPORTS



OPEN

Manipulating quantum information with spin torque

Brian Sutton & Supriyo Datta

Received: 27 September 2015

Accepted: 09 November 2015

Published: 09 December 2015

The use of spin torque as a substitute for magnetic fields is now well established for classical operations like the switching of a nanomagnet. What we are describing here could be viewed as an application of spin torque like effects to quantum processes involving single qubit rotations as well as two qubit entanglement. A key ingredient of this scheme is the use of a large number of itinerant electrons whose cumulative effect is to produce the desired qubit operations on static spins. Each interaction involves entanglement and collapse of wavefunctions so that the operation is only approximately unitary. However, we show that the non-unitary component of the operations can be kept below tolerable limits with proper design. As a capstone example, we present the implementation of a complete CNOT gate using the proposed spin potential based architecture, and show that the fidelity under ideal conditions can be made acceptably close to one.

There has been enormous progress in the field of spintronics in the last twenty-five years driven by the discovery of diverse new phenomena that have made it possible to generate and detect useful levels of non-equilibrium spin currents and spin potentials even at room temperature. Some of these phenomena are finding applications in memory devices, see for example¹, and a number of proposals have been put forth seeking to utilize them both for conventional logic and for neuromorphic logic^{2,3}. Since spin is a primary entity envisioned for the physical realization of quantum bits, or qubits^{4,5}, it seems natural to ask whether the modern advancements in generating non-equilibrium spin currents and voltages could be harnessed in building robust quantum computers.

One influential proposal for the design of a quantum computer^{5,6} is based on the use of donor and nuclear spins of phosphorous ³¹P atoms in a silicon matrix and much experimental progress has been reported in the last fifteen years towards the realization of structures that could enable proposals of this type^{7–10}. Single qubits, \vec{S} , are selected and rotated using magnetic fields, while two qubit operations are realized by activating an effective exchange interaction $J\vec{S}_1 \cdot \vec{S}_2$ between them.

The use of spin torque as a substitute for magnetic fields is now well established for classical operations like the switching of a nanomagnet. Our primary objective in this paper is to show that “spin torque” like effects can be used to implement quantum processes involving single qubit initialization and rotation as well as two qubit entanglement. Qubit readout using ensemble-measurement can be implemented using the same architecture if a collection of identically initialized and transformed qubits, prepared using replicated physical structures, are available for measurement. Alternatively the proposed architecture could be used in conjunction with established single shot readout techniques⁸, especially for specific applications requiring multi-qubit state tomography or Bell state experiments.

In this paper we will first show that (1) all standard single qubit operations can be effected without any magnetic field through interactions of the form $J\vec{\sigma} \cdot \vec{S}$ with the itinerant or “flying” non-equilibrium spin population $\vec{\sigma}$ while (2) two qubit operations can be implemented through separate interactions of the form $J\vec{\sigma} \cdot \vec{S}_1$ and $J\vec{\sigma} \cdot \vec{S}_2$ with the flying spin population $\vec{\sigma}$. The latter process has been discussed earlier by several authors^{11–21} and we draw on this work, but there is a key distinction with the present work as explained in the next section.

Materials and Methods

The overall architecture we envision is shown schematically in Fig. 1(a) using four localized spins for illustrative purposes. A complete implementation could include additional qubits as well as multiple versions of the same qubit to allow ensemble readout. All qubits are embedded in a spin-coherent semiconductor channel so that the itinerant or “flying” (f) spins in the conduction band interact with the static (S_i) qubits located at x_i through an interaction of the form

School of Electrical and Computer Engineering and Purdue Quantum Center, Purdue University, West Lafayette, IN, 47907. Correspondence and requests for materials should be addressed to B.S. (email: bmsutton@purdue.edu) or S.D. (email: datta@purdue.edu)

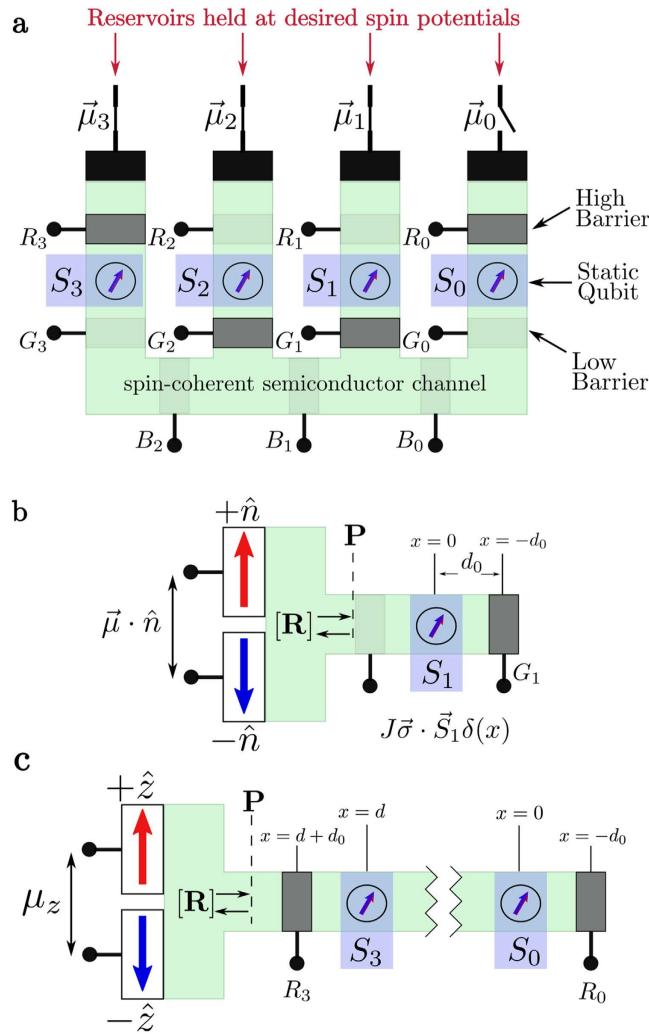


Figure 1. Quantum computing with “spin torque”. (a) Schematic showing the overall architecture with qubits S_1 and S_2 configured for single qubit operations and qubits S_0 and S_3 for two qubit operations. (b) Equivalent configuration for qubit S_1 redrawn in one dimension. (c) Equivalent configuration for qubits S_0 and S_3 redrawn in one dimension.

$$\mathcal{H} = J\vec{\sigma} \cdot \vec{S}_i \delta(x - x_i) \tag{1}$$

The static qubit could be a charge-neutral nuclear spin like ^{29}Si with J representing the hyperfine interaction, or ^{31}P where the donor level is used to mediate a hyperfine interaction, or it could be the electronic donor spin with J representing the exchange interaction, or perhaps a nanoscale magnet embedded in the semiconductor^{22,23}.

Each qubit has gates, R_i and G_i , on either side that can be used to deplete the channel underneath to couple and decouple the qubits from the itinerant spins as desired for specific operations. The spin-coherent channel has additional gates, B_i , that provide isolation and direct the flow of electrons. These gates could be realized using top-gates²⁴ or through contacts capable of modulating the electrostatics of the channel¹⁰. A general itinerant electron has a low probability of interacting with a static nuclear spin due to the minuscule size of the nucleus. In order to effect an interaction, the gates, R_i and G_i , are used to produce standing waves for the itinerant electrons. These standing waves should in-turn provide the necessary wavefunction overlap to realize the coupled interaction with a static spin²⁵.

The semiconducting channel could be realized using silicon²⁶ or other material supporting coherent spin injection and transport^{27,28}. Itinerant spins can be connected as desired to spin reservoirs held at specific spin potentials²⁹ along the x , y or z directions. These can be generated using various well-established spintronic phenomena such as magnetic contacts^{30,31}, the giant spin Hall effect^{32,33}, or spin pumping³⁴, at both low³⁵ and room temperatures^{36,37}. Integration of semiconductors with magnetic materials is a viable prospect^{38,39} and has been used in silicon double dot experiments to generate local magnetic fields⁴⁰, establishing precedent for the prospect of device fabrication. Please see the discussion section for additional discussion of these topics along with a summary of the essential requirements for the proposal in Table 1.

Requirement	Discussion
1. Spin-injection into semiconductors <i>Threshold:</i> $p > 0$ <i>Objective:</i> $p = 1.0$ <i>Precedent:</i> $p = 0.1\text{--}0.3$ in Si at 5 K ⁴⁷ $p = 0.046$ in n-Si at 300 K ³⁷	a. Polarization is highly temperature dependent b. Can compensate for low polarization (e.g. $p = 0.01$) through modulation of N via α if barrier height/position is tunable c. $p = 1.0$ is not a fundamental requirement for gate operations d. Heusler alloys may enable higher polarizations ³⁹ e. Two distinct spin-potentials ($\bar{\mu}$) needed for universality f. Polarized current not required for two-qubit operations
2. Coherent spin transport <i>Threshold:</i> $\lambda_S \propto d, d_0$ <i>Objective:</i> $\lambda_S = \infty$ <i>Precedent:</i> $\lambda_S \approx 10 \mu\text{m}$ in Si at 85 K ²⁶ $\lambda_S \approx 5 \mu\text{m}$ in graphene at room temp ²⁸	a. Minimum distance governed by proximity of qubits to each other and to neighboring barriers b. Low-temperatures best for long spin-coherence length c. Isotopically enriched semiconductor ideal for coherence d. Non-locality directly related to obtainable λ_S e. Small λ_S may still facilitate nearest-neighbor approaches f. Channel confinement necessary to ensure “1D” operation
3. Exchange/Hyperfine coupling between itinerant and static spins: $\mathcal{H} = J\vec{\sigma} \cdot \vec{S}_i \delta(x - x_i)$ <i>Precedent:</i> Nuclear polarization with spin-current ²⁵	a. ³¹ P donors ideal for Si, but interaction with donor electron warrants discussion b. Itinerant spins simultaneously coupled to static qubits may complicate this model c. Quasi-static model used to describe interaction d. Alternate qubits may fit into this model (e.g. quantum dots, nanomagnets)
4. Single-shot initialization and readout compatibility <i>Precedent:</i> ³¹ P donors in Si ^{7,8}	a. Spin polarization of 1.0 needed for fiducial state preparation b. Single-shot readout needed for correlation measurements and traditional implementations of quantum algorithms c. Architecture is compatible with demonstrated single-shot initialization and readout mechanisms d. Ensemble-measurement computing is inherently supported

Table 1. Essential Requirements. There are a number of requirements that must be satisfied in order for the proposed architecture to be viable. Shown in the table are a few of the most essential requirements for the proposal along with precedent for their satisfaction.

Figure 1(a) shows qubits S_1 and S_2 configured for single qubit operations and can be redrawn in one dimension as shown in Fig. 1(b). Qubits S_0 and S_3 on the other hand are configured for two qubit operations and can be redrawn as shown in Fig. 1(c). Note that in either case the two reservoirs shown are purely conceptual; in practice these would likely be a single reservoir with a spin potential $\bar{\mu}$ in some direction \hat{n} . With a single contact under steady-state conditions there is no net current flow, however there is a continual exchange of electrons. Electrons are preferentially injected from the contact with spins in direction \hat{n} which interact with the static qubits and are then removed by the same contact. It is this flow of electrons to and from the same contact that drives the scattering phenomena described in the following sections.

The density matrix of the incident spins from this reservoir is given by $\rho_f = [\mathbf{I} + \hat{n} \cdot \vec{\sigma}]/2$ where \mathbf{I} is the 2×2 identity matrix and $\vec{\sigma}$ the Pauli spin matrices. The Kronecker product of this flying spin density matrix with the $2^q \times 2^q$ density matrix ρ_s describing the q-qubit system ($q = 1$ for Fig. 1(b), $q = 2$ for Fig. 1(c)) gives the initial overall $2^{q+1} \times 2^{q+1}$ density matrix of the system. The initial density matrix gets modified to

$$\rho = [\mathbf{R}][\rho_f \otimes \rho_s][\mathbf{R}^\dagger] \quad (2)$$

by the reflection process described by a $2^{q+1} \times 2^{q+1}$ reflection matrix $[\mathbf{R}]$ which is computed taking into account the barrier(s) and the interaction of the itinerant spins with the qubits and depends on the specific structure at hand.

The reflected itinerant spins are returned to the spin reservoir ($+\hat{n}$ or $-\hat{n}$) causing a collapse of the quantum state described by a partial trace of the density matrix over the flying spins represented by Trace_f:

$$\rho_s(n+1) = \text{Trace}_f([\mathbf{R}][\rho_f \otimes \rho_s(n)][\mathbf{R}^\dagger]) \quad (3)$$

Equation (3) defines the basic approach we will use to model the quantum gates discussed in this paper. It provides a recursive relation expressing the q-qubit density matrix after interacting with $(n+1)$ itinerant spins in terms of the density matrix after interacting with n itinerant spins. A time-independent model for quantum transport is used assuming that the time variation of signals is slow enough to be treated as quasi-static. For example, $\hbar/1 \text{ ns} \approx 1 \mu\text{eV}$ which is much smaller than other energy scales of interest.

The use of “flying spins” to manipulate static qubits has been discussed in the past^{11–21} and it has been noted that the reflection matrix $[\mathbf{R}]$ in equation (2) represents a unitary transformation suitable for quantum operations if the barriers at $x = -d_0$ in Fig. 1(b,c) are large enough to reflect the incident electrons completely^{20,21}, which we employ in this proposal. What is new about the present proposal’s method is the use of sequential interactions with

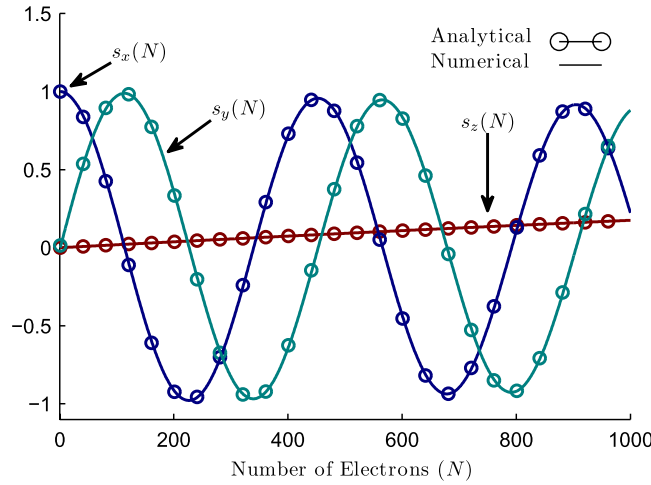


Figure 2. Single Qubit Rotation. Evolution of the spin of a single qubit initially pointing along x as it interacts with an increasing number of flying spins, N . The numerical results are described very well by the analytical solutions (4) and (5) described in the text.

a large number of itinerant electrons, each interaction involving a process of entanglement and reflection, equation (2), followed by a collapse, without post-selection, of the quantum state, equation (3), resulting in a deterministic, approximately unitary operation. Every interaction evolves the density matrix according to equation (3) which can be used iteratively to determine the final density matrix after interacting with a specified number of electrons.

Note that unlike equation (2), the collapse of the density matrix described by equation (3) is a non-unitary process and it may seem surprising that an overall operation involving a large number (N) of such non-unitary collapses could still be useful for implementing unitary transformations suitable for quantum computing. However, we will show that with proper choice of parameters the degree of non-unitarity can be made arbitrarily small at the expense of speed.

We seek to show that the non-unitarity that is inevitable with multiple collapses can be held to acceptably low levels so that useful quantum gates can be implemented. This is established first for single qubit operations and then for two qubit operations using the basic approach embodied in equations (2) and (3). Finally, as a capstone example, we present the implementation of a complete CNOT gate using the proposed architecture, and show that the fidelity under ideal conditions can be made acceptably close to one.

Results

Single Qubit Operations. Figure 1(b) shows the basic configuration for a single qubit operation: in the following discussion we will assume that \hat{n} points along the z -direction, so that the reservoir injects electrons with $+z$ spins and extracts both $\pm z$ spins. Every time an electron is injected it gets entangled with the static spin, while the extraction represents a measurement that collapses the quantum state of the static spin. We show in Supplementary Section A that after interaction with N electrons, the z -component of the static spin \bar{s} is given by

$$s_z(N) = 1 - (1 - s_z(0))(\cos \alpha)^{2N} \tag{4}$$

while the transverse component $s_t \equiv s_x + is_y$ is given by

$$s_t(N) = s_t(0)e^{iN\alpha}(\cos \alpha)^N \tag{5}$$

where α represents the effective interaction strength between the flying spin and the static qubit and is given by

$$\begin{aligned} \tan \alpha &= \frac{8\Omega \sin^2 kd_0}{1 - 2\Omega \sin(2kd_0) - 6\Omega(1 - \cos 2kd_0)} \\ &\rightarrow 8\Omega(kd_0)^2, \text{ if } kd_0 \ll 1 \end{aligned} \tag{6}$$

where k is the wavenumber of the itinerant electrons, v the corresponding velocity and

$$\Omega \equiv J/\hbar v \tag{7}$$

Equations (4) and (5) describe our numerical results accurately, as evident from Fig. 2, and provide the basis for single qubit initialization and rotation respectively as described in the discussion section.

Two Qubit Operations. Figure 1(c) shows the basic configuration for a two qubit operation which is very similar to that for a single qubit operation, Fig. 1(b), except that the channel has two embedded qubits instead of

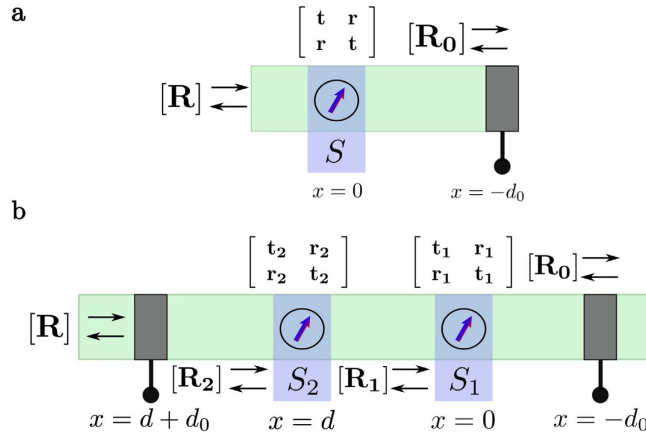


Figure 3. Single and Two Qubit Reflection Matrices. Reflection matrix $[R]$ for (a) single qubit operations and (b) two qubit operations.

one. The overall approach is the same, based on equation (3), but the reflection matrix $[R]$ is 8×8 in size instead of 4×4 , making the algebra less straightforward.

In the two qubit subspace we are seeking to implement a unitary transformation of the form

$$\begin{matrix} & 1\bar{2} & \bar{1}\bar{2} & \bar{1}\bar{2} & \bar{1}\bar{2} \\ \begin{matrix} 1\bar{2} \\ \bar{1}\bar{2} \\ \bar{1}\bar{2} \\ \bar{1}\bar{2} \end{matrix} & \begin{pmatrix} 1 & 0 & 0 & 0 \\ 0 & \cos \gamma & -i \sin \gamma & 0 \\ 0 & -i \sin \gamma & \cos \gamma & 0 \\ 0 & 0 & 0 & 1 \end{pmatrix} & & & \end{matrix} \quad (8)$$

which could be viewed as a “rotation” in the $1\bar{2} - \bar{1}\bar{2}$ space: a rotation of $\gamma = \pi/2$ corresponds to a SWAP while $\gamma = \pi/4$ corresponds to the universal $\sqrt{\text{SWAP}}$ operation that we will use for the CNOT gate.

The approach used is based on the general principle of using itinerant spins as “messengers” that interact with the static spins through separate terms of the form $J\vec{\sigma} \cdot \vec{S}_1, J\vec{\sigma} \cdot \vec{S}_2$. Each messenger causes a small rotation, and an overall rotation is achieved through the integrated effect of many messengers.

To see how this works we need the reflection matrix $[R]$ which is calculated using an extension of the method used in Supplemental Section A. The interaction with each of the qubits is described by transmission and reflection matrices given by

$$\mathbf{t}_1 = [\mathbf{I}_8 + i\Omega\tilde{\mathbf{S}}_1]^{-1} \text{ and } \mathbf{r}_1 = \mathbf{t}_1 - \mathbf{I}_8 \quad (9)$$

$$\mathbf{t}_2 = [\mathbf{I}_8 + i\Omega\tilde{\mathbf{S}}_2]^{-1} \text{ and } \mathbf{r}_2 = \mathbf{t}_2 - \mathbf{I}_8 \quad (10)$$

where $\tilde{\mathbf{S}}_1 = \vec{\sigma} \cdot \vec{S}_1$ and $\tilde{\mathbf{S}}_2 = \vec{\sigma} \cdot \vec{S}_2$ are 8×8 matrices (see Supplemental Section D for the explicit form of these matrices) describing the interactions of the itinerant spin with qubits 1 and 2 respectively. Note that the two qubit structure (Fig. 3(b)) has an additional barrier on the left with spin-independent transmission and reflection matrices given by

$$\mathbf{t}_B = \frac{1}{1 + i\Gamma} \mathbf{I}_8 \text{ and } \mathbf{r}_B = \mathbf{t}_B - \mathbf{I}_8 \quad (11)$$

where $\Gamma = U/\hbar v$ represents the barrier height normalized to $\hbar v$, assuming a delta function barrier $U\delta(x)$.

The overall reflection matrix $[R]$ is calculated by repeated cascade of the reflection matrices for the structure in Fig. 3(b).

$$\mathbf{R}_1 = \mathbf{r}_1 + e^{i2kd_0} \mathbf{t}_1 [\mathbf{I}_8 - e^{i2kd_0} \mathbf{R}_0 \mathbf{r}_1]^{-1} \mathbf{R}_0 \mathbf{t}_1 \quad (12)$$

$$\mathbf{R}_2 = \mathbf{r}_2 + e^{i2kd} \mathbf{t}_2 [\mathbf{I}_8 - e^{i2kd} \mathbf{R}_1 \mathbf{r}_2]^{-1} \mathbf{R}_1 \mathbf{t}_2 \quad (13)$$

$$\mathbf{R}_3 = \mathbf{r}_B + e^{i2kd_0} \mathbf{t}_B [\mathbf{I}_8 - e^{i2kd_0} \mathbf{R}_2 \mathbf{r}_B]^{-1} \mathbf{R}_2 \mathbf{t}_B \quad (14)$$

It is straightforward to use equations (12–14) to calculate the reflection matrix $[R]$ for a given set of parameters Ω, Γ, kd , and kd_0 .

Regardless of the detailed choice of parameters, the overall reflection matrix is block-diagonal. Two of these are trivial 1×1 blocks, $f1\bar{2}$ and $\bar{f} \bar{1}\bar{2}$, all upspin and all downspin, which remain unaffected by the interaction. The other two blocks are 3×3 blocks involving $f1\bar{2}, \bar{f}1\bar{2}, \bar{f} \bar{1}2$ and $\bar{f} \bar{1}\bar{2}, f1\bar{2}$ corresponding to (2 upspins + 1

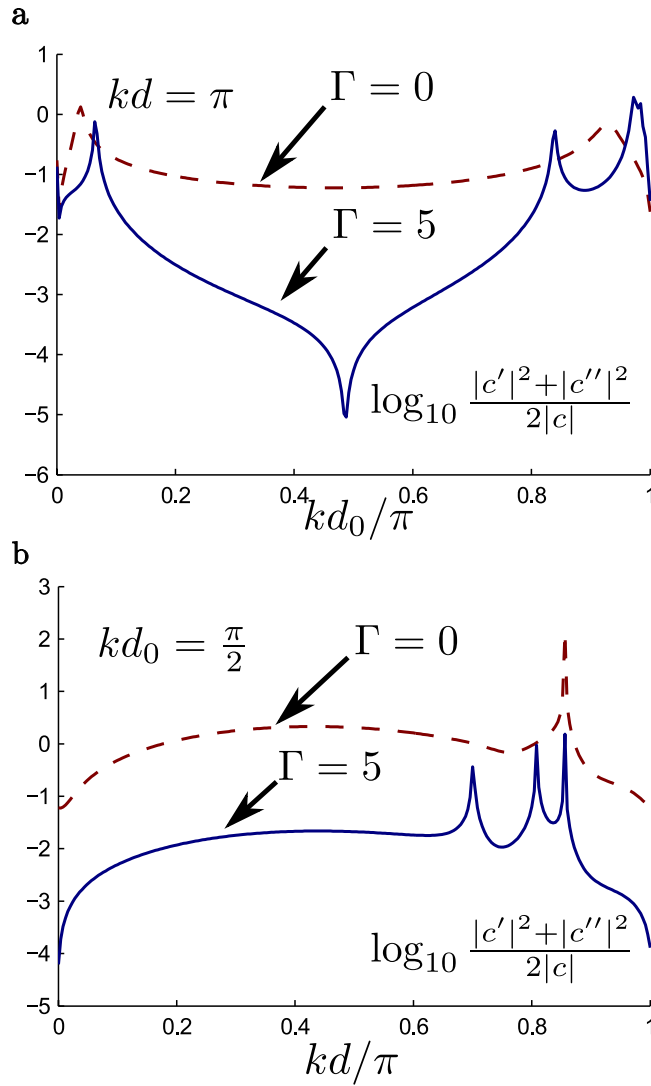


Figure 4. Figure of merit. Figure of merit for two qubit operations as a function of (a) kd_0 for $kd = \pi$ and (b) kd for $kd_0 = \pi/2$ with $\Omega = 1$ and $\Gamma = 0$ and $\Gamma = 5$.

downspin) and (1 upspin + 2 downspins) respectively. The overall block-diagonal reflection matrix $[\mathbf{R}]$ can be written in terms of five non-zero matrix elements a, b, c, c' and c'' as shown below:

$$[\mathbf{R}] : \begin{matrix} & f_{12} & f_{1\bar{2}} & f_{\bar{1}2} & f_{\bar{1}\bar{2}} & \bar{f}_{12} & \bar{f}_{1\bar{2}} & \bar{f}_{\bar{1}2} & \bar{f}_{\bar{1}\bar{2}} \\ \begin{matrix} f_{12} \\ f_{1\bar{2}} \\ f_{\bar{1}2} \\ f_{\bar{1}\bar{2}} \\ \bar{f}_{12} \\ \bar{f}_{1\bar{2}} \\ \bar{f}_{\bar{1}2} \\ \bar{f}_{\bar{1}\bar{2}} \end{matrix} & \begin{pmatrix} 1 & 0 & 0 & 0 & 0 & 0 & 0 & 0 \\ 0 & a & c & 0 & c' & 0 & 0 & 0 \\ 0 & c & a & 0 & c'' & 0 & 0 & 0 \\ 0 & 0 & 0 & b & 0 & c'' & c' & 0 \\ 0 & c' & c'' & 0 & b & 0 & 0 & 0 \\ 0 & 0 & 0 & c'' & 0 & a & c & 0 \\ 0 & 0 & 0 & c' & 0 & c & a & 0 \\ 0 & 0 & 0 & 0 & 0 & 0 & 0 & 1 \end{pmatrix} \end{matrix} \quad (15)$$

Note that if c', c'' were zero, our reflection matrix would nearly provide the transformation we are looking for with term c providing the two qubit rotation γ in equation (8). But the terms c' and c'' cause undesirable non-unitary effects leading to an average error probability

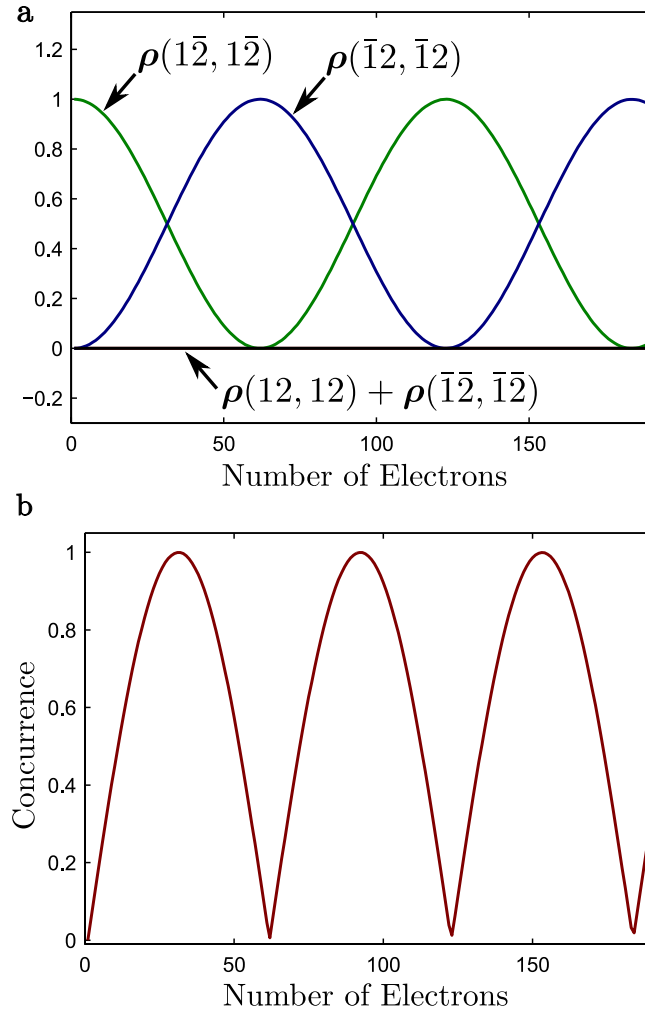


Figure 5. Two qubit rotation. (a) Two qubit rotation with $kd = \pi$, $kd_0 = \pi/2$, $\Omega = 0.1$, and $\Gamma = 20$. (b) Two qubit concurrence showing the oscillation of entanglement as a function of the number of incident electrons.

$$P_e \sim (|c'|^2 + |c''|^2)/2$$

so that the error probability per unit rotation for the two qubit gate can be estimated from

$$\frac{P_e}{\theta} \sim \frac{|c'|^2 + |c''|^2}{2|c|} \tag{16}$$

which is plotted in Fig. 4 as function of kd and kd_0 assuming $\Omega \equiv J/\hbar v = 1$, $\Gamma = 5$. Note that with

$$kd = \pi \text{ and } kd_0 \approx \pi/2$$

the error probability is quite small $\sim 10^{-4}$.

To illustrate the importance of adding the additional semi-transparent barrier of strength Γ in front, we have also shown the results without it ($\Gamma = 0$) in dashed lines which show much larger error probability.

Figure 5(a) shows the evolution of the diagonal elements of the density matrix as it interacts with itinerant spins starting from an initial state with $\rho(1\bar{2}, 1\bar{2}) = 1$. Note that entangled states with very high concurrence, see equation (10) from⁴¹, are obtained with the proper number of electrons (Fig. 5(b)).

CNOT Implementation. We end this section with an example of another universal two qubit quantum gate, the CNOT, implemented using the spin potential-based architecture described here. Figure 6(a) shows a CNOT gate in terms of elementary single qubit and two qubit operations⁴. The circuit can be realized using the basic structure shown in Fig. 1(a) gated appropriately to obtain two qubits embedded in a spin coherent channel. These qubits can be selectively connected or disconnected from contacts held at specified spin potentials.

The timing diagram in Fig. 6(c) shows the sequence of single qubit and two qubit operations needed to implement the required gate:

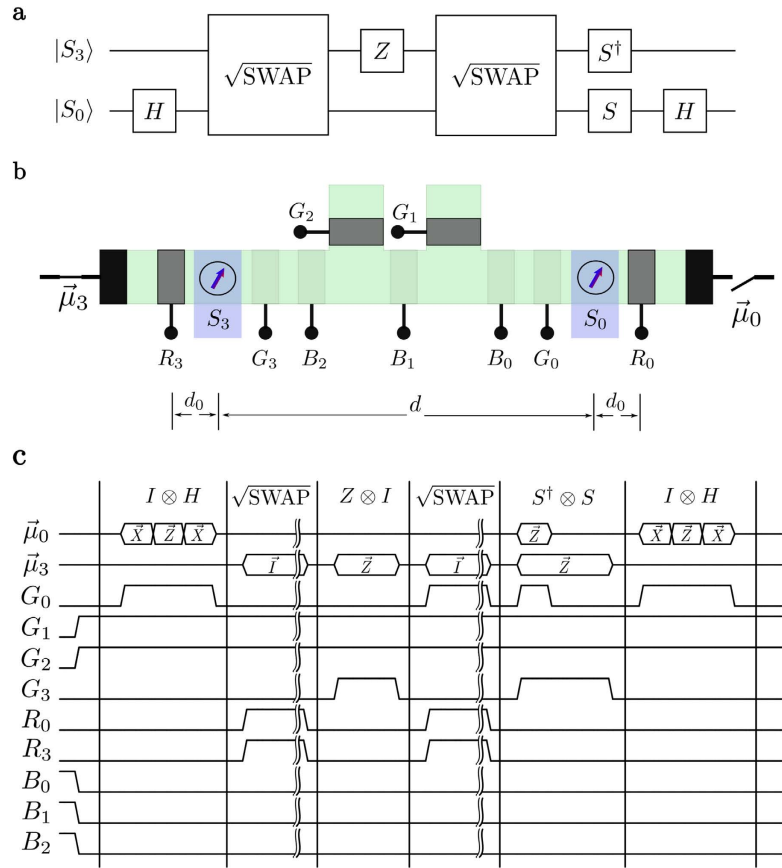


Figure 6. Controlled-NOT. (a) Circuit representation for CNOT based on the controlled-Z with Hadamard gates to obtain a controlled-X. (b) Physical picture for single and two qubit operations on $|S_0\rangle$ and $|S_3\rangle$ with electrostatically controlled gates. (c) Waveforms depicting the manipulations necessary for the various nets of Fig. (b) to perform a CNOT operation between $|S_0\rangle$ and $|S_3\rangle$.

1. H-gate: This involves $\pi/2$ rotations of $|S_0\rangle$ around the x, z, and x axes in sequence. The barrier gates G_i, R_i and B_i are used to isolate $|S_0\rangle$ which is then rotated by connecting the $\vec{\mu}_0$ terminal to reservoirs with x and z-directed spin potentials, each for the length of time needed to provide the $\pi/2$ rotation.
2. $\sqrt{\text{SWAP}}$ gate: This involves a two qubit rotation on $|S_0\rangle$ and $|S_3\rangle$ of the type discussed in the previous section. This gate is realized with the use of an unpolarized spin potential for the length of time appropriate for a $\pi/4$ “rotation” (eq. (8)). Note the use of barrier gates R_0 and R_3 to implement the completely reflective barrier and the semitransparent barrier respectively.
3. Z-gate: This rotation of qubit $|S_3\rangle$ around the z-axis is achieved by using gate G_3 for isolation and then connecting to a z-directed spin potential for an appropriate duration.
4. $\sqrt{\text{SWAP}}$ gate: same as step 2.
5. S and S^\dagger gates: This involves a $\pi/2$ rotation of $|S_0\rangle$ and a $3\pi/2$ rotation of $|S_3\rangle$, both around the z-axis.
6. H-gate: same as step 1.

The complete CNOT gate was simulated with single qubit and two qubit operations as described earlier with $\Omega = \pi/16$ and $\Gamma = 10^2$. A 0.5% error in the desired values of kd and kd_0 was assumed:

$$kd = 0.995\pi \text{ and } kd_0 = 0.995\pi/2$$

The fidelity of the gate was estimated using the prescription laid out by Trifunovic *et al.*⁴². The CNOT gate was simulated with each of the four $((1/\sqrt{2})(|01\rangle \pm |11\rangle)$ and $(1/\sqrt{2})(|00\rangle \pm |10\rangle))$ initial states that give rise to Bell states, and the fidelity of the final state ρ' was evaluated by comparing to the ideal Bell state ρ :

$$f(\rho, \rho') = \sqrt{\sqrt{\rho}\rho'\sqrt{\rho}} \tag{17}$$

The minimum value of f was 99.8%.

Discussion

Given the results of the previous section, we will assess the viability of the single and two qubit operations for fault tolerant quantum computing. After establishing the validity of these operations, we will then reflect on various aspects of the overall architecture.

Single Qubit Operations.

Single qubit initialization. Equation (4) tells us that a static spin can be initialized in a state with $s_z \rightarrow 1$, after interaction with a large number of flying spins ($N \rightarrow \infty$). This is similar to the well-known Overhauser effect whereby nuclear spins get polarized through interaction with a spin reservoir driven out of equilibrium^{25,43} or other proposals for state purification using repeated measurements of a coupled quantum system with post-selection^{44–46}.

Single qubit rotation. Equation (5) suggests the possibility of single qubit rotation by an angle $\theta = N\alpha$ around the z-axis through interaction with the itinerant spins. Note, however, that in the process the spin is also attenuated by a factor $(\cos \alpha)^N$ which is an undesirable side effect. For a given total rotation $\theta = N\alpha$ we can write the resulting error probability per unit rotation as

$$\frac{P_e}{\theta} = \frac{1}{\theta} \left(1 - \left(\cos \frac{\theta}{N} \right)^N \right) \approx \frac{\theta}{2N}, \text{ if } \frac{\theta}{N} \ll 1 \quad (18)$$

which shows that P_e can be made arbitrarily small for a given rotation θ by choosing a large N and hence a small α . The results in Fig. 2 were obtained with a relatively large value of α with $N \sim 100$ spins for a rotation of $\theta = \pi/2$ in order to make the non-unitary effects apparent with a large error probability. But with $N \sim 10^4$, we have an error probability $P_e \sim 1.23 \times 10^{-4}$.

The use of a large N also gives enhanced control over the process since each electron makes only a small difference to the result. A large N requires a small α , and equation (6) suggests a convenient mechanism for the control of α , namely by adjusting the effective distance d_0 of the reflective barrier through the barrier voltage.

In this discussion, the polarization of the magnetic contact, \hat{n} , was taken as 100% in the z-direction. In practice, the polarization $P = (N_{\text{up}} - N_{\text{dn}})/(N_{\text{up}} + N_{\text{dn}})$ will be less than 100%. The angle of rotation will then be determined by $N_{\text{up}} - N_{\text{dn}}$, while the non-unitarity will depend on $N_{\text{up}} + N_{\text{dn}}$, making the error probability in equation (18) larger by $(1/P)$. For example, a spin polarization of 0.01 would increase the error probability by 10^2 . In order to compensate for this increase in error, we would need $(1/P)$ times more electrons, $N' = P^{-1}N$, which could be accomplished by making α smaller. In silicon, spin polarizations an order of magnitude larger than 0.01 have been obtained at low temperatures⁴⁷ with promising progress at room temperature³⁵.

Single qubit readout. Note that the interaction we just discussed also provides a mechanism for readout if we have multiple replicas of each qubit available so that ensemble measurements can be made, similar to¹⁷. We could measure the average spin current I_{sz} that flows initially at the terminals

$$(I_{sz})_{N=0} = \frac{dN}{dt} \frac{ds_z}{dN}_{N=0} = (1 - s_z(0)) \frac{dN}{dt} 2 \ln \cos \alpha \quad (19)$$

and deduce $s_z(0)$ from it. Similarly the initial spin in the x- and y-directions can be obtained by measuring the spin current that flows when connected to a spin reservoir with an x- and y-component respectively and using equations (4, 5). Knowing $s_i(0)$, $i = x, y, z$, we can write down the initial density matrix as follows:

$$\rho = \frac{1}{2} [\mathbf{I} + s_x(0)\sigma_x + s_y(0)\sigma_y + s_z(0)\sigma_z] \quad (20)$$

Ensemble measurement techniques provide a mechanism to obtain the expectation value of a given qubit and may be useful for certain computations⁴⁸. However, as the architecture is compatible with single-shot readout methods, replicated physical structures are a non-essential aspect of the proposal.

Two Qubit Operations. The direct approach to implementing a two qubit rotation is through an interaction of the form $\vec{S}_1 \cdot \vec{S}_2$ between the two static spins as, for example, in the Kane architecture⁵ or more recently in the quantum dot approaches proposed by Trifunovic et al.^{42,49}. Using the proposed itinerant spin approach to mediate an effective exchange interaction leads to an inherent imperfection in the gate operations. These imperfections arise as a result of the undesirable coefficients c' and c'' of (15) due to the interactions $\vec{\sigma} \cdot \vec{S}_1, \vec{\sigma} \cdot \vec{S}_2$. This is apparent if we compare the matrix representation of these operators with $[\mathbf{R}]$ in equation (15). On the other hand, the desirable coefficient c arises from product terms of the form

$$[\vec{\sigma} \cdot \vec{S}_1][\vec{\sigma} \cdot \vec{S}_2] + [\vec{\sigma} \cdot \vec{S}_2][\vec{\sigma} \cdot \vec{S}_1]$$

which are independent of the spin of the itinerant electrons, $\vec{\sigma}$, so that the two qubit operation, unlike the single qubit operations, does not require a spin potential; an ordinary unpolarized reservoir should be fine. The lack of phase symmetry of Eq. (15) for up and down flying spins, and hence imperfection in the $\sqrt{\text{SWAP}}$, is somewhat

mitigated with the use of un-polarized itinerant spins as, on average, the $|12\rangle$ and $|\bar{1}\bar{2}\rangle$ states will pick up the same overall phase.

The fidelity of the two-qubit $\sqrt{\text{SWAP}}$ gate is strongly dependent on the height of the initial barrier, Γ . For $\Gamma \neq 0$, the enhancement in gate fidelity, being due to multiple reflection, is wavelength dependent, and hence k dependent. At low temperatures the relevant k is the Fermi wavevector k_f corresponding to the Fermi energy which is related to the electron density n_s ⁵⁰:

$$k_f = \sqrt{2\pi n_s} \quad (21)$$

In general, however, a thermal average over wavevectors is involved and the degree of enhancement from multiple reflections will be averaged accordingly.

It should also be noted that since the reduced error probability with $\Gamma \neq 0$ comes from multiple coherent reflections, this gain in performance can be expected to be more sensitive to processes that cause a loss of spin coherence. Such processes are ignored in our present model.

Finally, the fidelity of the complete CNOT implementation of 99.8% is sufficient for fault tolerant quantum computing⁴².

Architecture. The proposed architecture has a number of features that may be advantageous for building a quantum computer in semiconductor based architectures. The itinerant spins generate localized magnetic fields for any target qubit, providing individual qubit selectivity, parallel operation, and qubit isolation. This localized field generation removes the need for AC electric and magnetic fields used for nuclear magnetic resonance (NMR) and electron spin resonance (ESR). Removing the need for these magnetic fields reduces the complexity of system design for qubit manipulation.

External DC magnetic fields can be eliminated if perfect half-metallic contacts can be obtained to produce 100% spin polarized currents suitable for high-fidelity qubit initialization. These ideal spin currents are currently difficult to realize experimentally, and an alternative initialization method is needed in the near-term. Alternatively, this architecture is compatible with existing approaches that leverage an external magnetic field to produce Zeeman splitting such that single qubit initialization and readout can be accomplished with single electron transistors.

Using itinerant spins for gate operations must be compatible with the decoherence times of the qubits. There have been significant recent advances in the long-term storage of quantum information in semiconductor systems based around donor and defect spins with experimental results of ³¹P nuclear spin T_2 times ~ 30 seconds²⁴, and high-purity silicon donor electrons with T_2 times \sim seconds^{51,52}. These long decoherence times are much greater than the operation time of the quantum gates driven by itinerant spins: a current of 160 nA can deliver 10^4 electrons, sufficient for a qubit rotation, in ~ 10 ns. Spin lifetimes of over 500 ns at 60 K have been reported in undoped Si⁵³.

While single qubit gates in the architecture require the use of spin polarized currents and hence the integration of magnetic materials, two qubit gates can be realized with traditional contacts that produce un-polarized spin currents. Furthermore, these two qubit gates can be used to obtain non-local entanglement between selective qubits, a limitation of nearest neighbor proposals. The degree of non-locality will be limited by the spin coherent transport length of the itinerant quasi-particles which, depending on the material and the temperature, can range from tens of nanometers to tens of microns. However, coupling to channel contacts along with multiple reflections from barriers, increasing the effective transport length of the itinerant spins, will limit their range. As long as spin coherence can be maintained over a gate length (see Fig. 1) between two qubits, it should be possible to entangle them.

The use of a large number of itinerant spins to effect a given qubit operation allows fine tuning and control since a deviation of one electron represents a small error in a process involving, say, 10^4 electrons. We envision controlling the actual number of electrons using gates to connect or disconnect the qubits from the itinerant spins as desired. The use of all-electrical control of qubits is beneficial for producing a scalable architecture using semiconductor based qubits. Other proposals for all-electrical control exist, however, these proposals are largely based on spin-orbit interactions and are likely to be susceptible to charge noise⁵⁴.

Many proposals for qubit manipulations require sensitive gate control and the ability to manipulate single electrons. Here, the control for gate operations is based on a large number of electrons drawn from a reservoir which can be controlled accurately. Additionally, the architecture does not require a bound donor electron to perform nuclear spin manipulation which may provide a path for higher temperature operation⁵⁵. As a further example of the reduction in control necessary to implement the architecture, the gate operations do not require precise placement of donors in the lattice.

Nevertheless, there are a number of challenges that are incurred by the architecture. Prominently is the inherent loss of gate fidelity as a result of repeated measurement. This loss of gate fidelity requires error correction even before other sources of decoherence and dephasing are considered. Magnetic material integration into semiconductor processing is another obstacle that must be overcome for experimental realization of high-fidelity initialization, single qubit gates, and ensemble qubit readout. There has been progress towards integration of these materials into fabrication processes as a result of modern magnetic memory technologies, however, this integration is still emerging and does not have mainstream adoption. Additionally, an interaction of the form given by (1) was assumed throughout the proposal. Based on this assumption, a more detailed exploration of the interaction between conduction-band flying electrons and donor-based nuclear spins is warranted.

In summary, we have outlined a quantum computing architecture based on the use of non-equilibrium spin potentials enabled by modern spintronics to perform all basic qubit operations including initialization, arbitrary single qubit rotation, single qubit readout, and two qubit rotation on selected pairs of qubits. A key feature of our architecture is the use of repeated entanglement with itinerant electrons and a subsequent collapse of the quantum state. The latter process is non-unitary, but we have shown that the overall non-unitary component can

be kept below tolerable limits with proper design. Finally we presented the implementation of a complete CNOT gate using the proposed spin potential based architecture, and showed that the fidelity under ideal conditions is acceptable for fault tolerant quantum computing. This all-electrical architecture provides a means of qubit control for semiconductor donor systems without the use of magnetic fields while providing qubit selectivity and isolation, and non-local two qubit operation. Future research may include further investigation of the two qubit entanglement operation, numerical modeling of representative experimental structures, and investigation of the interaction between conduction band flying electrons and donor-based nuclear spins. Experimental investigation of the operations described herein would be valuable to assess the validity of the proposal.

References

- Chen, E. *et al.* Advances and future prospects of spin-transfer torque random access memory. *IEEE Trans. Magn.* **46**, 1873–1878 (2010).
- Locatelli, N., Cros, V. & Grollier, J. Spin-torque building blocks. *Nature Mater.* **13**, 11–20 (2014).
- Behin-Aein, B., Wang, J.-P. & Wiesendanger, R. Computing with spins and magnets. *MRS Bulletin* **39**, 696–702, doi: 10.1557/mrs.2014.166 (2014).
- Loss, D. & DiVincenzo, D. P. Quantum computation with quantum dots. *Phys. Rev. A* **57**, 120–126 (1998).
- Kane, B. E. A silicon-based nuclear spin quantum computer. *Nature* **393**, 133–137 (1998).
- Skinner, A. J., Davenport, M. E. & Kane, B. E. Hydrogenic spin quantum computing in silicon: a digital approach. *Phys. Rev. Lett.* **90**, 087901 (2003).
- Pla, J. J. *et al.* A single-atom electron spin qubit in silicon. *Nature* **489**, 541–545 (2012).
- Pla, J. J. *et al.* High-fidelity readout and control of a nuclear spin qubit in silicon. *Nature* **496**, 334–338 (2013).
- Zwanenburg, F. A. *et al.* Silicon quantum electronics. *Rev. Mod. Phys.* **85**, 961–1019 (2013).
- Büch, H., Mahapatra, S., Rahman, R., Morello, A. & Simmons, M. Y. Spin readout and addressability of phosphorus-donor clusters in silicon. *Nature Commun.* **4**, 2017 (2013).
- Costa, A. T., Bose, S. & Omar, Y. Entanglement of two impurities through electron scattering. *Phys. Rev. Lett.* **96**, 230501 (2006).
- Ciccarello, F., Palma, G. M., Zarcone, M., Omar, Y. & Vieira, V. R. Electron Fabry-Perot interferometer with two entangled magnetic impurities. *J. Phys. A: Math. Theor.* **40**, 7993 (2007).
- Yuasa, K. & Nakazato, H. Resonant scattering can enhance the degree of entanglement. *J. Phys. A: Math. Theor.* **40**, 297 (2007).
- Ciccarello, F., Paternostro, M., Kim, M. S. & Palma, G. M. Extraction of singlet states from noninteracting high-dimensional spins. *Phys. Rev. Lett.* **100**, 150501 (2008).
- Ciccarello, F., Paternostro, M., Palma, G. M. & Zarcone, M. Reducing quantum control for spin-spin entanglement distribution. *New J. Phys.* **11**, 113053 (2009).
- Yuasa, K. Extraction of an entanglement by repetition of the resonant transmission of an ancilla qubit. *J. Phys. A: Math. Theor.* **43**, 095304 (2010).
- De Pasquale, A., Yuasa, K. & Nakazato, H. State tomography of a qubit through scattering of a probe qubit. *Phys. Rev. A* **80**, 052111 (2009).
- Yuasa, K., Burgarth, D., Giovannetti, V. & Nakazato, H. Efficient generation of a maximally entangled state by repeated on- and off-resonant scattering of ancilla qubits. *New J. Phys.* **11**, 123027 (2009).
- Cordourier-Maruri, G. *et al.* Implementing quantum gates through scattering between a static and a flying qubit. *Phys. Rev. A* **82**, 052313 (2010).
- Ciccarello, F. *et al.* Quasideterministic realization of a universal quantum gate in a single scattering process. *Phys. Rev. A* **85**, 050305 (2012).
- Pasquale, A. D., Ciccarello, F., Yuasa, K. & Giovannetti, V. Selective writing and read-out of a register of static qubits. *New J. Phys.* **15**, 043012 (2013).
- Tejada, J., Chudnovsky, E. M., del Barco, E., Hernandez, J. M. & Spiller, T. P. Magnetic qubits as hardware for quantum computers. *Nanotechnology* **12**, 181–186 (2001).
- Khajetoorians, A. A. *et al.* Current-driven spin dynamics of artificially constructed quantum magnets. *Science* **339**, 55–59 (2013).
- Muhonen, J. T. *et al.* Storing quantum information for 30 seconds in a nanoelectronic device. *Nature Nanotech.* **9**, 986–991 (2014).
- Trowbridge, C. J., Norman, B. M., Kato, Y. K., Awschalom, D. D. & Sih, V. Dynamic nuclear polarization from current-induced electron spin polarization. *Phys. Rev. B* **90**, 085122 (2014).
- Appelbaum, I., Huang, B. & Monsma, D. J. Electronic measurement and control of spin transport in silicon. *Nature* **447**, 295–298 (2007).
- Koo, H. C. *et al.* Control of spin precession in a spin-injected field effect transistor. *Science* **325**, 1515–1518 (2009).
- Gao, Y., Kubo, Y., Lin, C.-C., Chen, Z. & Appenzeller, J. in *Electron Devices Meeting (IEDM) 2012 IEEE Int. 4.4.1-4.4.4*, doi: 10.1109/IEDM.2012.6478978 (2012).
- Brataas, A., Bauer, G. E. W. & Kelly, P. J. Non-collinear magnetoelectronics. *Phys. Rep.* **427**, 157–255 (2006).
- Fiederling, R. *et al.* Injection and detection of a spin-polarized current in a light-emitting diode. *Nature* **402**, 787–790 (1999).
- Schmidt, G. Concepts for spin injection into semiconductors— a review. *J. Phys. D: App. Phys.* **38**, R107 (2005).
- Seki, T. *et al.* Giant spin Hall effect in perpendicularly spin-polarized FePt/Au devices. *Nature Mater.* **7**, 125–129 (2008).
- Liu, L. *et al.* Spin-torque switching with the giant spin Hall effect of tantalum. *Science* **336**, 555–558 (2012).
- Kaestner, B. *et al.* Single-parameter quantized charge pumping in high magnetic fields. *Appl. Phys. Lett.* **94**, 012106 (2009).
- Jansen, R. Silicon spintronics. *Nature Mater.* **11**, 400–408 (2012).
- Jiang, X. *et al.* Highly spin-polarized room-temperature tunnel injector for semiconductor spintronics using MgO(100). *Phys. Rev. Lett.* **94**, 056601 (2005).
- Dash, S. P., Sharma, S., Patel, R. S., de Jong, M. P. & Jansen, R. Electrical creation of spin polarization in silicon at room temperature. *Nature* **462**, 491–494 (2009).
- van't Erve, O. M. J. *et al.* Low-resistance spin injection into silicon using graphene tunnel barriers. *Nature Nano* **7**, 737–742 (2012).
- Farshchi, R. & Ramsteiner, M. Spin injection from Heusler alloys into semiconductors: a materials perspective. *J. Appl. Phys.* **113**, 191101 (2013).
- Wu, X. *et al.* Two-axis control of a singlet-triplet qubit with an integrated micromagnet. *Proc. Natl. Acad. Sci.* **111**, 11938–11942 (2014).
- Wootters, W. K. Entanglement of formation of an arbitrary state of two qubits. *Phys. Rev. Lett.* **80**, 2245–2248 (1998).
- Trifunovic, L. *et al.* Long-distance spin-spin coupling via floating gates. *Phys. Rev. X* **2**, 011006 (2012).
- Overhauser, A. W. Polarization of nuclei in metals. *Phys. Rev.* **92**, 411–415 (1953).
- Nakazato, H., Takazawa, T. & Yuasa, K. Purification through Zeno-like measurements. *Phys. Rev. Lett.* **90**, 060401 (2003).
- Nakazato, H., Unoki, M. & Yuasa, K. Preparation and entanglement purification of qubits through Zeno-like measurements. *Phys. Rev. A* **70**, 012303 (2004).
- Militello, B., Yuasa, K., Nakazato, H. & Messina, A. Influence of dissipation on the extraction of quantum states via repeated measurements. *Phys. Rev. A* **76**, 042110 (2007).

47. Jonker, B. T., Kioseoglou, G., Hanbicki, A. T., Li, C. H. & Thompson, P. E. Electrical spin-injection into silicon from a ferromagnetic metal/tunnel barrier contact. *Nature Phys.* **3**, 542–546 (2007).
48. Boykin, P. O., Mor, T., Roychowdhury, V. & Vatan, F. Algorithms on ensemble quantum computers. *Nat. Comp.* **9**, 329–345 (2009).
49. Trifunovic, L., Pedrocchi, F. L. & Loss, D. Long-distance entanglement of spin qubits via ferromagnet. *Phys. Rev. X* **3**, 041023 (2013).
50. Datta, S. *Electronic Transport in Mesoscopic Systems* (Cambridge University Press, Cambridge, 1997).
51. Tyryshkin, A. M. *et al.* Electron spin coherence exceeding seconds in high-purity silicon. *Nature Mater.* **11**, 143–147 (2012).
52. Steger, M. *et al.* Quantum information storage for over 180 s using donor spins in a ²⁸Si 'semiconductor vacuum'. *Science* **336**, 1280–1283 (2012).
53. Huang, B., Monsma, D. J. & Appelbaum, I. Coherent spin transport through a 350 micron thick silicon wafer. *Phys. Rev. Lett.* **99**, 177209 (2007).
54. Nadj-Perge, S., Frolov, S. M., Bakkers, E. P. A. M. & Kouwenhoven, L. P. Spin-orbit qubit in a semiconductor nanowire. *Nature* **468**, 1084–1087 (2010).
55. Saeedi, K. *et al.* Room-temperature quantum bit storage exceeding 39 minutes using ionized donors in silicon-28. *Science* **342**, 830–833 (2013).

Acknowledgements

It is a pleasure to acknowledge Dr. Rajib Rahman and Rifat Ferdous for helpful discussions throughout the course of this work. This work also benefited from discussions with Dr. Bhaskaran Muralidharan and Dr. Behtash Behin-Aein. S.D. was supported by the Center for Science of Information (CSoI), an NSF Science and Technology Center, under grant agreement CCF-0939370. Numerical computations were performed using nanoHUB.org computational resources, part of the Network for Computational Nanotechnology (NCN).

Author Contributions

B.S. and S.D. jointly wrote the main manuscript text and prepared figures. Both reviewed the manuscript.

Additional Information

Supplementary information accompanies this paper at <http://www.nature.com/srep>

Competing financial interests: The authors declare no competing financial interests.

How to cite this article: Sutton, B. and Datta, S. Manipulating quantum information with spin torque. *Sci. Rep.* **5**, 17912; doi: 10.1038/srep17912 (2015).



This work is licensed under a Creative Commons Attribution 4.0 International License. The images or other third party material in this article are included in the article's Creative Commons license, unless indicated otherwise in the credit line; if the material is not included under the Creative Commons license, users will need to obtain permission from the license holder to reproduce the material. To view a copy of this license, visit <http://creativecommons.org/licenses/by/4.0/>